PERGAMON

International Journal of Solids and Structures 37 (2000) 1191–1209

INTERNATIONAL JOURNAL OF SOLIDS and STRUCTURES

www.elsevier.com/locate/ijsolstr

Effects of periodic and localized imperfections on struts on nonlinear foundations and compression sandwich panels

M. Ahmer Wadee*

Department of Mechanical Engineering, University of Bath, Claverton Down, Bath BA2 7AY, UK

Received 6 May 1998; in revised form 2 September 1998

Abstract

Heuristic studies of a strut on an elastic foundation and a strut with a sinusoidally varying load are extended to include initial geometric imperfections. Examination of various shapes of imperfection leads to the conclusion that for the majority of cases the most severe form is localized to a section of the structure rather than periodically distributed along the length. This leads to an examination of the imperfection sensitivity of an axially-loaded sandwich panel, the geometry of which is determined from a simple optimization routine bringing together two distinct modes of buckling. It is found that such a structure exhibits highly unstable snap-back behaviour in the perfect case and that combined with localized imperfections, it would never attain its linear critical buckling load.

1. Introduction

Recent work on the localization of buckle patterns has led to greater understanding of structural systems that undergo subcritical instability (Champneys et al., 1997). Although these studies have mainly been concerned with the perfect systems, insight of the qualitative behaviour of imperfect systems can be readily obtained merely by examining their initial stability characteristics. An axially-loaded rectangular long plate supported on all edges exhibits supercritical instability, periodic buckle patterns, and is stable in the post-buckling range, implying that an imperfect plate is not very sensitive to initial imperfections in the elastic range; any imperfection sensitivity of the plate is usually associated with yielding. The classic counter-example is a system that exhibits localized buckling, an axially-loaded cylindrical shell for instance, which is severely unstable in the elastic post-buckling range (Lord et al., 1997) and so can be assumed to be highly imperfection sensitive. However, in systems where localization occurs the detailed

* Present address: Department of Civil and Environmental Engineering, Imperial College of Science, Technology and Medicine, London, SW7 2BU, UK. Fax: 00 44 207 225 2716.

E-mail address: a.wadee@ic.ac.uk (M.A. Wadee).

0020-7683/00/$ - see front matter
PII: S0020-7683(98)00280-7

treatment of imperfections, whose shape sympathize with the final buckle pattern of the perfect system, has been somewhat constrained by a lack of suitable tools. Now, with the advent of powerful analytical and numerical tools such as symbolic computation and parameter continuation packages, such investigations are possible.

This paper extends this work on localization by introducing imperfections to three models, each of which exhibits localized buckling at some stage. Unlike classical work on imperfection sensitivity where there tends to be a unique worst case wavelength for the imperfection, the localization phenomenon forces the worst case imperfection to change shape as load changes. Earlier work used the strut on a nonlinear foundation and applied various shapes of imperfection to the system (Amazigo et al., 1970). The effects of the various imperfections were compared against each other by using the maximum amplitude of imperfection as the relative measure; this prejudices the results as periodic imperfections locally have identical maximum deflection but globally have many extrema at the same amplitude, whereas the localized imperfections have one extremum at that amplitude, implying a smaller *total* deflection. Naturally, the worst case was found to be the periodic type imperfection. Further work on similar lines was applied to the von Kármán-Donnell equations for the axially-loaded cylindrical shell (Amazigo and Fraser, 1971) and was later extended by Lucena Neto (1992).

In the present study, two types of imperfection (purely periodic and modulating localized) are examined on three separate systems. These are put into the following increasingly complex systems. The first is a linear strut on a softening nonlinear foundation with a constant compressive load (Hunt et al., 1989). The second is a linear strut on a softening nonlinear foundation with a sinusoidally varying load—the body force model (Hunt and Wadee, 1998); this qualitatively behaves as a system where there is an interaction with overall and local buckling modes (Thompson and Hunt, 1973; 1984). The third system results from a full interactive buckling formulation of a structural sandwich panel (Hunt and Wadee, 1998; Wadee and Hunt, 1998a), in which overall and local buckling interact to induce localized buckling.

The examination of imperfection sensitivity of the sandwich panel combines the study of the effects of structural optimization, as the panel is optimized by virtue of coinciding critical modes of buckling with the use of composite construction. Structural optimization has been popular over the years and especially so in the aeronautics industry (Prager, 1968; Steven et al., 1998) where composite materials and construction are used extensively (Mróz, 1970; Kodiyalam et al., 1996). Previous work on the effects of optimization in nonlinear structures (Thompson and Hunt, 1973; Budiansky, 1976) have highlighted the need for care in such designs so that complex instability is not promoted; the present work underlines this caution for designers of compression sandwich panels.

2. Development of the imperfect heuristic systems

This section formulates the differential equations for two heuristic models of struts on nonlinear elastic Winkler-type foundations, Fig. 1(a). The first is a strut on a softening quadratic foundation with a constant axial load, and the second model is a strut on a softening quadratic foundation but with a sinusoidally varying axial load. Both are modelled with a generalized imperfection, w_0, which is formulated from an energy principle. The nonlinear elastic foundation is chosen as softening to promote localization, and quadratic to investigate initial post-buckling. The form of the imperfection closely matches that of least stable localized buckling for the strut on a softening foundation—derived from a first order approximation of a multiple scale perturbation analysis (Wadee et al., 1997)

$$w_0(x) = A_0 \operatorname{sech}\big[\alpha(x-\psi)\big] \cos\big[\beta\pi(x-\psi)/L\big], \tag{1}$$

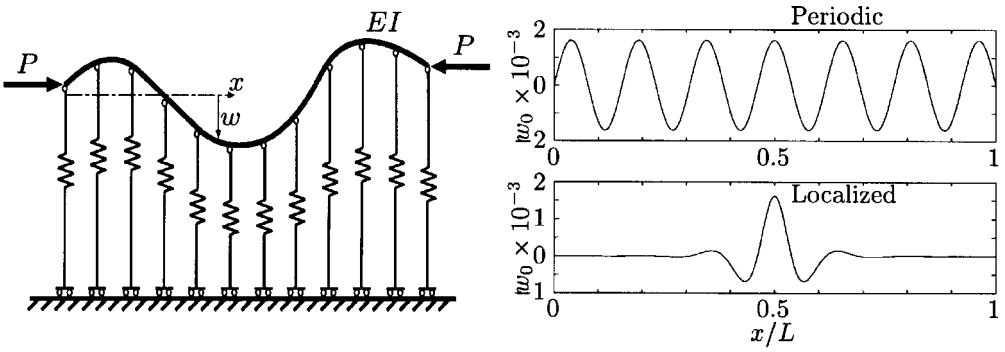

Fig. 1. The imperfect strut on an elastic foundation.

where $x \in [0, L]$ and w_0 is symmetric about $x = \psi$. This enables the study of periodic and localized imperfections; w_0 is periodic when $\alpha = 0$ with a wave number β, but has a modulated amplitude for $\alpha \neq 0$ (Fig. 1(b)).

2.1. Strut with constant load

The imperfection is introduced by supposing an initially deformed shape $w_0(x)$ is stress-relieved, such that the elemental bending moment, M, and thus stored strain energy of bending drop to zero as represented in Fig. 2 (Thompson and Hunt, 1984):

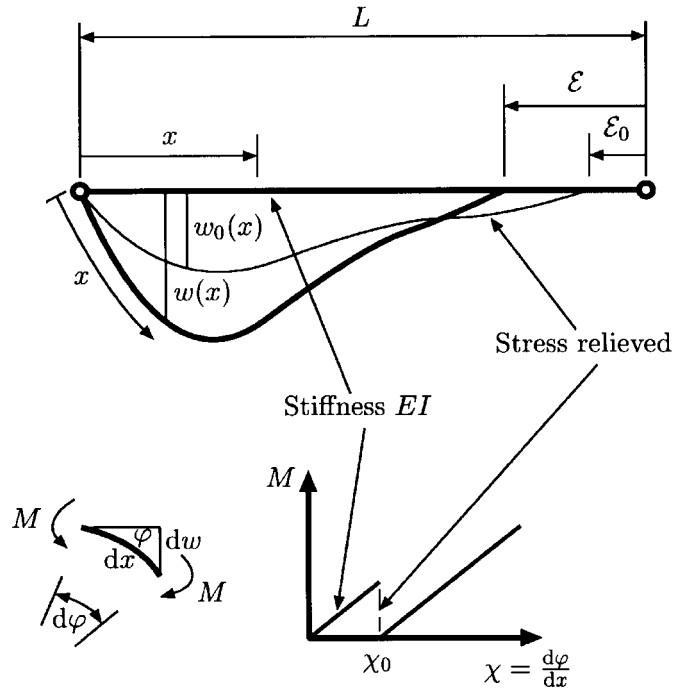

Fig. 2. Stress-relieved state of the strut, after Thompson and Hunt (1984).

$$\mathrm{d}U_\mathrm{b} = \frac{1}{2}M\,\mathrm{d}\varphi = \frac{1}{2}EI(\mathscr{K} - \mathscr{K}_0)^2\,\mathrm{d}x \tag{2}$$

where $\mathscr{K}$ is the curvature of the strut due to w. This also assumes that the strain energy in the foundation is non-zero in the initial state. Assuming a small deflection curvature relationship, i.e. $\mathscr{K} = w''$, the strain energy of bending becomes:

$$U_\mathrm{b} = \frac{1}{2}EI\int_0^L \left(w'' - w_0''\right)^2\,\mathrm{d}x, \tag{3}$$

where primes represent differentiation with respect to the spatial variable x. Including U_b into the total potential energy, V, along with the contributions of foundation energy and work done by the load P, the expression of V becomes:

$$V = \int_0^L \left[\frac{1}{2}EI\left(w'' - w_0''\right)^2 + \frac{1}{2}kw^2 - \frac{1}{3}k_1w^3 - \frac{1}{2}Pw'^2\right]\mathrm{d}x, \tag{4}$$

where k and k_1 respectively represent the linear and quadratic components of the constitutive law of the foundation F:

$$F = kw - k_1w^2 \tag{5}$$

Applying the calculus of variations to this functional, the following nonhomogeneous differential equation is obtained:

$$EIw'''' + Pw'' + kw - k_1w^2 = EIw_0'''' \tag{6}$$

This system has a propensity to buckle anywhere along the length. Thus the location of maximum imperfection should not change the limit load of the structure (except perhaps near a boundary).

2.2. Strut with sinusoidally varying load

This has the same imperfection formulation as above except the load term has an additional sinusoidal component as if the strut is already buckling in an overall (Euler-type) mode.

$$P_\mathrm{total} = P + Q\sin\frac{\pi x}{L} \tag{7}$$

Putting P_total into V (eqn (4)) instead of P and applying the calculus of variations, we obtain the following differential equation (Hunt and Wadee, 1998):

$$EIw'''' + Pw'' + Q\left(\sin\frac{\pi x}{L}w'' + \frac{\pi}{L}\cos\frac{\pi x}{L}w'\right) + kw - k_1w^2 = EIw_0''''. \tag{8}$$

This system would tend to buckle at midspan—the sinusoidal body force represented by Q places the maximum stress there.

3. Axially-compressed sandwich panel

Structural sandwich panels, Fig. 3, are used in applications where weight efficiency has to be combined with high strength. However, owing to the fact that they are efficient carriers of load in

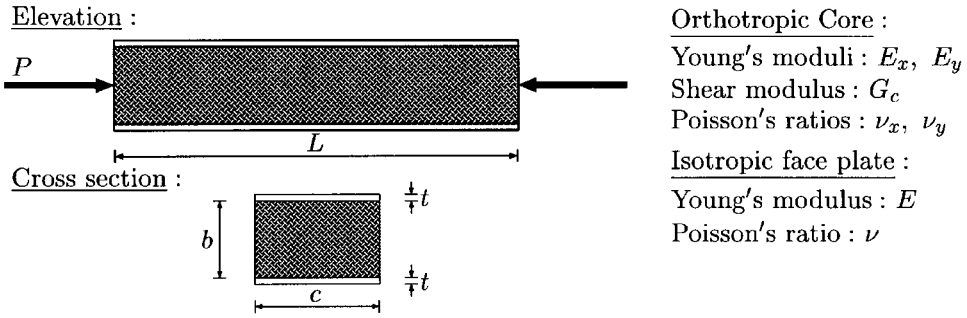

Fig. 3. Typical sandwich panel, cross-section and material properties.

compression, they tend to exhibit nonlinear mode interaction effects (Thompson and Hunt, 1973) involving an overall mode of buckling combined with a local mode of buckling on one face; localized buckling on one face is the result—leading to highly unstable post-buckling behaviour (Hunt and Wadee, 1998).

In this section, the linear critical load formulation for each of the distinct buckling modes is summarized, followed by an abridged presentation of the formulation of the model to describe the sandwich panel's post-buckling behaviour. This lays the foundation for the numerical case study where a simple optimization routine is employed to obtain an efficient panel. This panel is examined in detail for its perfect and imperfect post-buckling behaviour.

3.1. Critical buckling loads

The critical loads for overall and local buckling for the sandwich panel are derived from linear periodic Rayleigh–Ritz analyses (Allen, 1969; Hunt et al., 1988). For overall buckling, the core cannot be modelled by a Winkler-type foundation as this would implicitly assume the Euler–Bernoulli approximation that plane sections remain plane, denying shearing strains; this makes the face plates independent, and stops the possibility of local buckling. Thus, the effect of shearing in the core is accounted for by decomposing the overall half sine wave mode into separate sway and tilt components (Fig. 4). For the local mode, a straight combination of snake (anti-symmetric with shearing) and hourglass (symmetric and no associated shear) modes with an associated wave number i is employed such that one face remains unbuckled whilst the other face buckles periodically. Sway and tilt overall

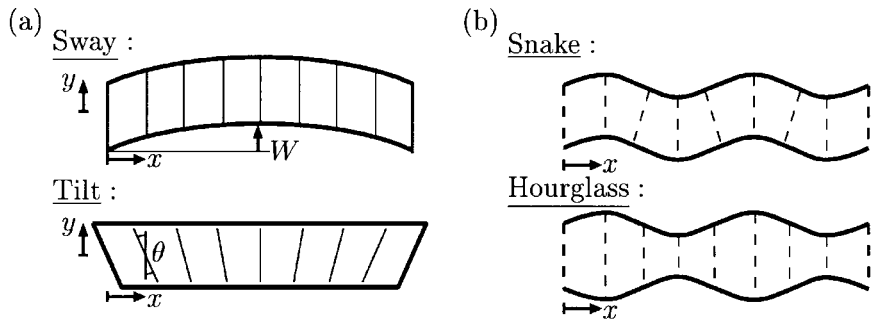

Fig. 4. Decomposed modes for critical buckling: (a) sway and tilt components of overall mode; (b) snake and hourglass modes of local buckling.

mode components W and θ with respective amplitudes q_s and q_t:

$$W(x) = q_s L \sin\frac{\pi x}{L}, \quad \theta(x) = q_t \pi \cos\frac{\pi x}{L}. \tag{9}$$

Snake (N) and hourglass (H) modes for local buckling:

$$W_N(x) = a_1 L \sin\frac{i\pi x}{L}, \quad \theta_N(x) = a_2 \pi \cos\frac{i\pi x}{L}, \quad W_H(x) = a_3 L \sin\frac{i\pi x}{L}. \tag{10}$$

Note that when one face remains straight, and the other face buckles periodically, $a_1 = a_3$.

3.1.1. Strain energy

Standard expressions suffice in the development of the different components of strain energy. Bending energy depends on the curvature ($\mathscr{K}$) of the panel faces as buckling takes place, membrane energy accounts for the direct stresses on the face plates, and core energy accounts for the two-dimensional stress state in the core consisting of both direct and shearing stresses. Table 1 contains all the necessary expressions for performing the linear analysis to obtain the overall and local critical buckling loads, where Δ is end-shortening arising from pure compression.

Total strain energy of bending, where EI is the flexural rigidity of one face plate:

$$U_b = \int_0^L EI\mathscr{K}^2 \, dx. \tag{11}$$

Membrane energy of both face plates:

$$U_m = \int_0^L \frac{1}{2} Etc\left[\varepsilon_x(x, b/2)^2 + \varepsilon_x(x, -b/2)^2\right] dx. \tag{12}$$

Strain energy stored in an orthotropic core under plane stress (Wadee and Hunt, 1998a):

$$U_c = \int_0^L \int_{-b/2}^{b/2} \left[\frac{c}{2(1 - v_x v_y)} \left(E_x \varepsilon_x^2 + E_y \varepsilon_y^2 + 2 v_x E_y \varepsilon_x \varepsilon_y \right) + \frac{G_c c}{2} \gamma_{xy}^2 \right] dy \, dx \tag{13}$$

and finally, the work done by the load is $P\varepsilon$. Therefore the total potential energy, V, is:

$$V = U_b + U_m + U_c - P\varepsilon \tag{14}$$

Applying linear eigenvalue analysis to the respective functionals for the overall and local buckling cases yields the respective critical loads for P:

Table 1
Strains (axial: ε, shear: γ), curvature ($\mathscr{K}$) and end-shortening (ε) expressions for linear energy formulation

	Overall mode	Local mode
ε_x	$-y\theta' - (1/2L)\int_0^L W'^2 \, dx - \Delta$	$-y\theta_N' - (1/2L)\int_0^L [(\partial/\partial x)(W_N + (2y/b)W_H)]^2 \, dx - \Delta$
ε_y	0	$(2/ib)W_H$
γ_{xy}	$W' - \theta$	$W_N' - \theta_N + (2y/b)W_H'$
$\mathscr{K}^2$	W''^2	$W_N''^2 + W_H''^2$
ε	Δ	Δ

$$P_{\mathrm{o}}^{\mathrm{C}} = \frac{2\pi^2 EI}{L^2} + \frac{2Gb^2\pi^2}{L^2}\left[\frac{\left(D + \frac{C_x}{6}\right)}{2G + \frac{b^2\pi^2}{L^2}\left(D + \frac{C_x}{6}\right)}\right], \tag{15}$$

$$P_{\mathrm{l}}^{\mathrm{C}} = K\left[\frac{2\pi^2 EIi^2}{L^2} + \frac{kL^2}{\pi^2 i^2} + \frac{4G}{3} - \frac{2G^2}{\frac{\pi^2 i^2 b^2}{L^2}\left(D + \frac{C_x}{6}\right) + 2G}\right], \tag{16}$$

where $P_{\mathrm{o}}^{\mathrm{C}}$ and $P_{\mathrm{l}}^{\mathrm{C}}$ are the overall and local buckling loads respectively, and:

$$EI = \frac{Ect^3}{12(1-\nu^2)}, \quad K = \frac{6Et(1-\nu_x\nu_y) + 3E_{\mathrm{c}}b}{6Et(1-\nu_x\nu_y) + 2E_{\mathrm{c}}b}, \quad D = \frac{Etc}{2}, \quad G = \frac{G_{\mathrm{c}}cb}{2} \tag{17}$$

$$k = \frac{E_y c}{2(1-\nu_x\nu_y)b}, \quad C_x = \frac{E_x bc}{2(1-\nu_x\nu_y)}. \tag{18}$$

3.2. Post-buckling and imperfections

The linear critical buckling analysis gives no indication of the true behaviour of the panel after buckling. A periodic Rayleigh–Ritz energy model taking the concept of the snake and hourglass modes a stage further, including the von Kármán large displacement expressions (Hunt et al., 1988), highlights the potential unstable nature of the post-buckling response (Fig. 5). As the overall modal amplitude grows, the neutral post-buckling path of an initial overall buckle is destabilized at a secondary bifurcation point, triggering an interactive local mode with a certain combination of the snake and hourglass forms. The effect of the secondary bifurcation is to reduce the load capacity of the panel. A wave number i can be determined for the worst case interaction—where the critical and secondary bifurcations are closest. Although this periodic post-buckling model highlights potentially destabilizing

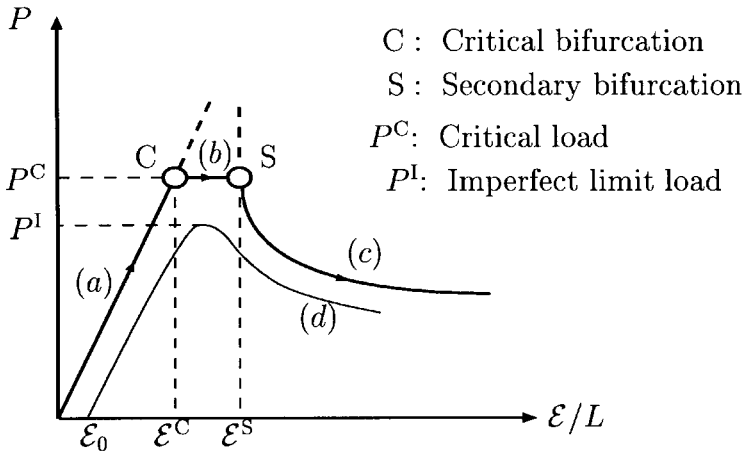

Fig. 5. Equilibrium diagram for sandwich panels: (a) fundamental path; (b) critical path of overall buckling; (c) secondary path of interactive buckling; (d) imperfect path.

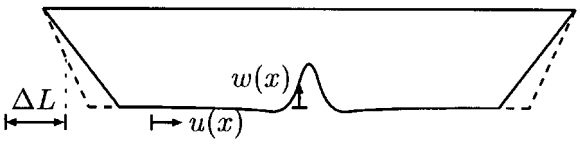

Fig. 6. Displacement functions used to describe interactive buckling.

secondary bifurcations, the periodicity is prescribed; what is needed is a post-buckling model with no such predefined buckle pattern—a variational model derived from energy to define the governing equations of the sandwich panel.

This general localized model (Hunt and Wadee, 1998; Wadee and Hunt, 1998a) develops a system of nonlinear differential equations that account for the interaction between overall and local modes of buckling of the sandwich panel and lead to a secondary instability on one face of the panel when the overall mode forces the effective load at midspan to exceed the local buckling load. Localized buckling is triggered as the periodicity of the local buckle gains a long wave modulation from the interaction with the overall mode. Formulation of the model requires two functions, $w(x)$ and $u(x)$, introduced to describe, respectively, lateral and in-plane deflections of the face that localizes (Fig. 6).

The governing equations are developed from the energy functional V after including new terms from the contributions to the energy of the functions w and u. The detailed derivation of the differential equations from the energy functional via the calculus of variations is found in Wadee and Hunt (1998a) for the case of an orthotropic core; resulting equations are stated including the imperfection, the analysis being aided by the symbolic computation package Maple V (Heck, 1996):

$$\begin{aligned} &EIw'''' + D\left[2\Delta w'' + q_t\frac{b\pi^2}{L}\left(\sin\frac{\pi x}{L}w'' + \frac{\pi}{L}\cos\frac{\pi x}{L}w'\right)\right. \\ &\left. - \left(2u''w' + 2u'w'' + 3w'^2w''\right)\right] + G\left[\frac{u'}{b} - \frac{2}{3}w'' + (q_s - q_t)\frac{\pi^2}{L}\sin\frac{\pi x}{L}\right] \\ &+ C_x\left[\frac{2}{3}\Delta w'' - \left(\frac{1}{2}u''w' + \frac{1}{2}u'w'' + \frac{3}{5}w'^2w''\right) + q_t\frac{b\pi^2}{6L}\left(\sin\frac{\pi x}{L}w'' + \frac{\pi}{L}\cos\frac{\pi x}{L}w'\right)\right] \\ &+ C_y\left[\frac{2}{3}v_x\left(ww'' + w'^2\right) - v_x\left(u' + \frac{1}{3}w'^2\right) - \frac{2}{3}v_x^2\Delta bw''\right] + kw = EIw_0'''', \end{aligned} \tag{19}$$

$$\left(D + \frac{C_x}{3}\right)u'' - \frac{G}{2b}\left(\frac{2}{b}u - w'\right) + \left(D + \frac{C_x}{4}\right)w'w'' - \frac{C_yv_x}{2}w' - \frac{G\pi}{b}\cos\frac{\pi x}{L}\left[(q_s - q_t) - \frac{q_t}{s}\right] = 0. \tag{20}$$

Eqns (19) and (20) respectively describe the lateral and in-plane deflection of the face plate under greater compression. The imperfection w_0 is introduced only to one face and in the same way as for the struts of the previous section. With w_0 present, the equilibrium path is smoothed with bifurcations being rounded off (Fig. 5(d)), with the maximum load, the limit load P^I, always less than the critical load from linear analysis P^C.

The differential equations are also subject to the following integral constraints, determined by minimizing V with respect to the generalized coordinates q_s, q_t and Δ (Hunt and Wadee, 1998):

$$P = \frac{2\pi^2 EI}{L^2} + \frac{2G}{q_s}\left[(q_s - q_t) + \frac{1}{\pi L}\int_0^L \cos\frac{\pi x}{L}\left(w' - \frac{2}{b}u\right) \mathrm{d}x\right], \tag{21}$$

$$s(q_s - q_t) = q_t + \int_0^L \left[\frac{s}{\pi L}\cos\frac{\pi x}{L}\left(\frac{2}{b}u - w'\right) - \frac{1}{b\pi^2}\sin\frac{\pi x}{L}\left(u' + \frac{1}{2}w'^2\right)\right] \mathrm{d}x, \tag{22}$$

$$\Delta = \frac{P + \int_0^L \left[\frac{2D}{L}\left(u' + \frac{1}{2}w'^2\right) + \left(\frac{C_x - C_y b v_x^2}{L}\right)\left(u' + \frac{1}{3}w'^2\right)\right] \mathrm{d}x}{4D + 2C_x - 2C_y v_x^2 b}, \tag{23}$$

where additional quantities are defined:

$$C_y = \frac{kb}{2}, \quad s = \frac{2GL^2}{b^2\pi^2}\left(D + \frac{C_x}{6}\right)^{-1}. \tag{24}$$

The panel is assumed to be simply-supported, eqn (25), and matching the applied stress at the ends gives the in-plane boundary conditions, eqn (26):

$$w(0) = w''(0) = w(L) = w''(L) = 0, \tag{25}$$

$$-\frac{P}{4D} = \left(1 + \frac{C_x}{3D}\right)u'(x_0) + \left(1 + \frac{C_x}{4D}\right)\frac{1}{2}w'^2(x_0) - \left(1 + \frac{C_x}{2D} - \frac{C_y v_x^2 b}{2D}\right)\Delta. \tag{26}$$

4. Numerical results

Each system formulated above has been studied extensively and results are presented below. For the first two, periodic imperfections are compared with worst case localized imperfections. The worst case is defined as the imperfection that minimizes the limit load for a given imperfect end-shortening ε_0; chosen as a more reasonable basis for comparison than used by Amazigo et al. (1970). Then the location of the maximum for the localized imperfection is varied such that it no longer occurs at midspan; the effects of varying ψ are quantified by how it changes the limit load.

For the third system, the compression sandwich panel, a linear optimization scheme is implemented. The resulting optimum panel is examined in the post-buckling range in both perfect and imperfect forms. Brief discussion on the use of optimization in systems which encounter subcritical bifurcations follows. These studies require the use of numerical parameter continuation techniques. A suitable package AUTO (Doedel et al., 1995) was implemented, using it as a boundary value problem solver in conjunction with its powerful capabilities for continuation and bifurcation problems in ordinary differential equations.

4.1. Periodic versus localized imperfection

4.1.1. Constant load strut

The differential equation for the strut on a softening quadratic foundation is in a nondimensional form

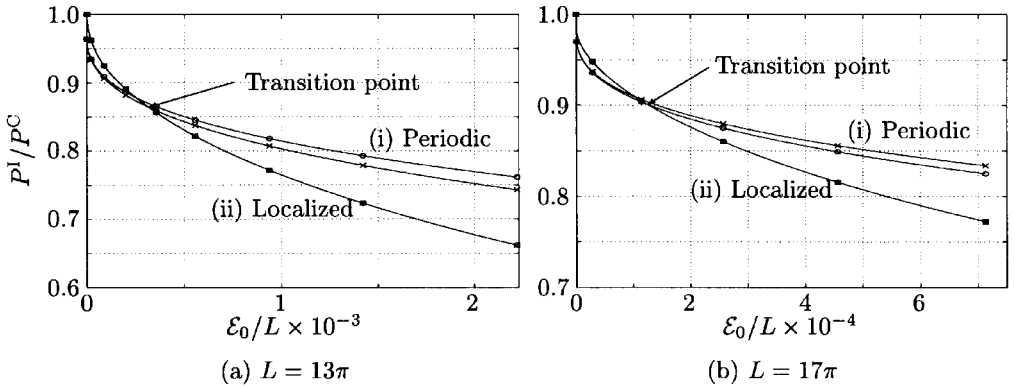

Fig. 7. Imperfection-sensitivity diagram for strut showing limit loads for (i) periodic imperfection (ii) most severe localized imperfection; where: (○)—constant β from linear eigenvalue analysis, (X)—variable β to minimize P^I.

$$w'''' + pw'' + w - w^2 = w_0'''', \tag{27}$$

where $p = P/\sqrt{kEI}$ from the original formulation and $p^C = 2$. Fig. 7(a) compares a periodic imperfection with a localized one (Fig. 1b). The periodic imperfection is examined in two stages. In the first, A_0 is varied while β is kept at the linear eigenvalue solution—L $= 13\pi$ implies $\beta = 13$. In the second stage, A_0 and β are both varied such that ε_0 is kept constant where

$$\varepsilon_0 = \int_0^L \frac{1}{2} w_0'^2 \, \mathrm{d}x. \tag{28}$$

Although ε_0 has a physical interpretation of strut end-shortening, it can also be thought as a mean square measure of the total initial imperfection. Similarly, the localized imperfection is examined in two stages. In the first, A_0 and α are changed while β is kept at the linear eigenvalue solution. Once a worst case combination of A_0 and α have been defined, the second stage holds ε_0 and α constant, while A_0 and β are adjusted to minimize the limit load. It is found that the limit load from the periodic imperfection can be significantly reduced by adjusting β slightly away from the eigenvalue solution, but in the localized case adjusting β does not make any significant change to the limit load.

A noteworthy feature is the transition of the type of worst case imperfection from periodic ($0 \leqslant \varepsilon_0/L \lesssim 0.35 \times 10^{-3}$) to localized. This is hypothesized to be connected with the length dependence of the perfect strut—the secondary bifurcation triggering localization not coinciding with the critical bifurcation in finite length struts (Hunt et al., 1989). Furthering this investigation lead to Figs. 7(b) and 8 where the transition occurs earlier for a longer strut, and the locus of transition points is shown for a spread of lengths respectively; the hypothesis seems to be confirmed:

$$L \to \infty \Longrightarrow \varepsilon^S \to \varepsilon^c, \left(P^I/P^C\right)_{\text{trans}} \to 1, \quad (\varepsilon_0)_{\text{trans}} \to 0. \tag{29}$$

4.1.2. Body force strut

Similarly for the body force strut in a nondimensional form,

$$w'''' + pw'' + q\left(\sin\frac{\pi x}{L} w'' + \frac{\pi}{L}\cos\frac{\pi x}{L} w'\right) + w - w^2 = w_0'''', \tag{30}$$

where $q = Q/\sqrt{kEI}$, for different values of q, imperfections are compared against each other with the

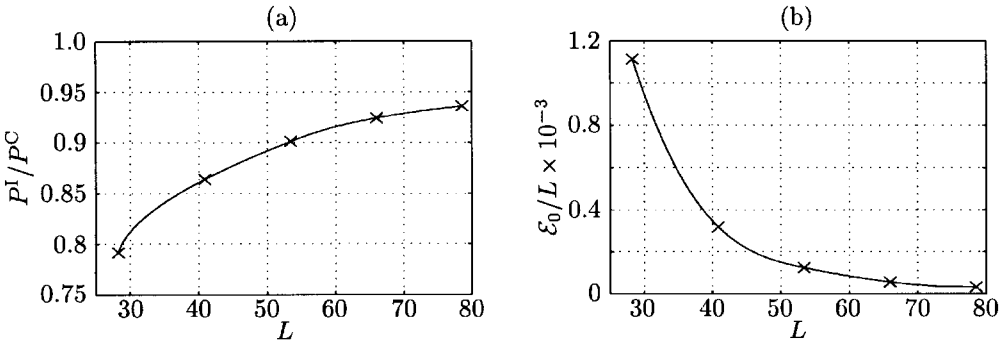

Fig. 8. Locus of points showing the transition where the worst case imperfection changes from periodic to localized: (a) limit loads against strut length; (b) initial imperfection end-shortening against strut length.

same procedure as for the constant load strut. Like the localized imperfections in the constant load case, the difference in the limit loads when β is constant and when β is varied is hardly distinguishable, but this time for both periodic and localized imperfections.

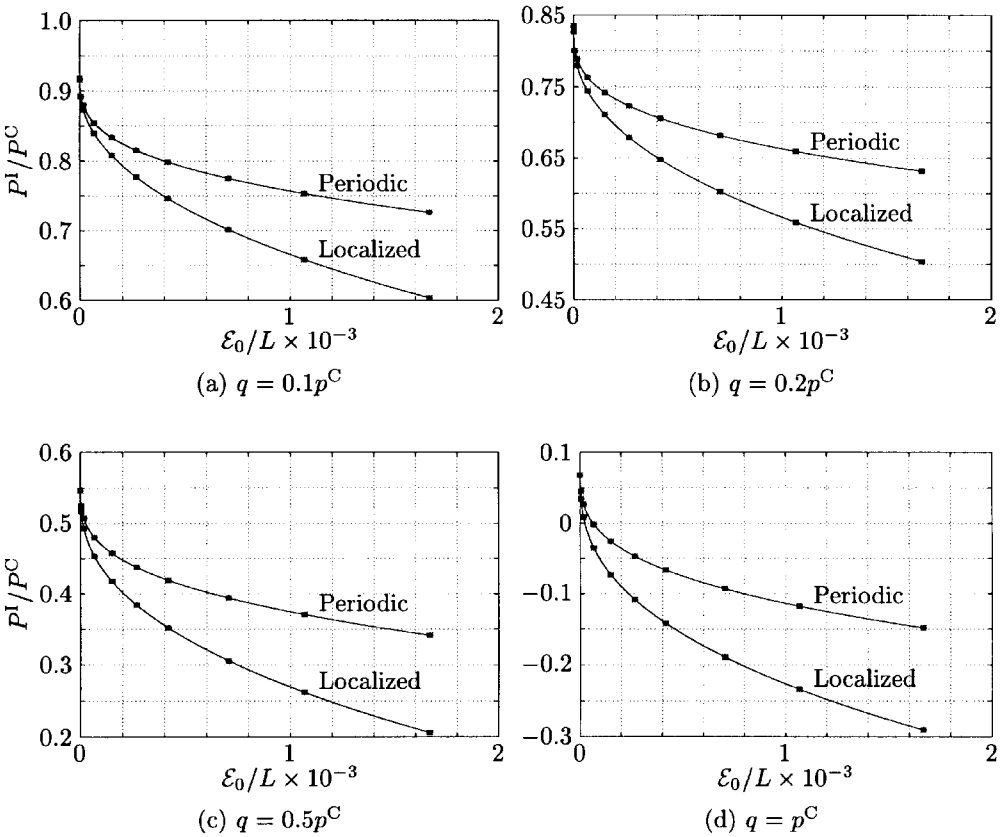

Fig. 9. Imperfection sensitivity diagrams for body force strut with varying q.

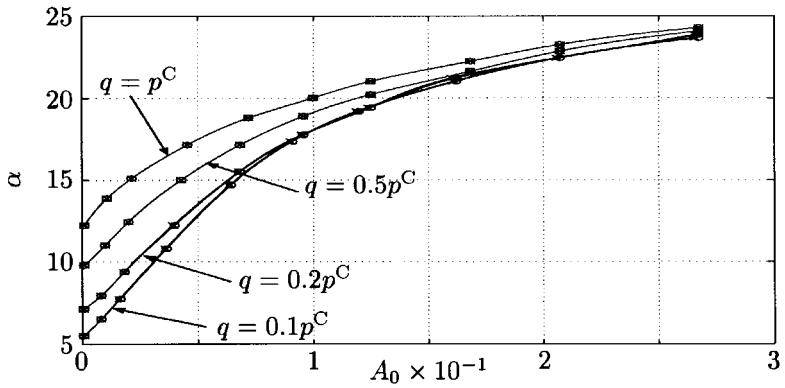

Fig. 10. Variation of worst case combinations of A_0 and α for the body force strut imperfection with different q values.

Fig. 9 shows imperfection sensitivity curves for the cases of $q = 0.1\,p^C$, $q = 0.2\,p^C$, $q = 0.5\,p^C$ and $q = p^C$, where $p^C = 2$. These curves show that, unlike the constant load case, the localized imperfection is always the worst case for $q > 0$. Fig. 10 shows the variation of the worst case A_0 and α as ε_0 increases. This shows that the initial values of α are quite different. However, as ε_0 increases, the worst case combinations of A_0 and α for the separate cases seem to converge on to one path.

4.2. Location of maximum imperfection

In the previous section the location of the maximum imperfection is set at midspan. In the following, ψ is varied to see how this affects limit load, P^I. Fig. 11 shows exactly how the imperfection is changed along the length.

Fig. 12(a) shows the limit load variation as the imperfection is shifted along the length for the constant load strut. It shows that only when the boundary affects the shape of the imperfection—by causing A_0 to increase, as ε_0 remains constant—the limit load changes. Therefore, for long struts, where

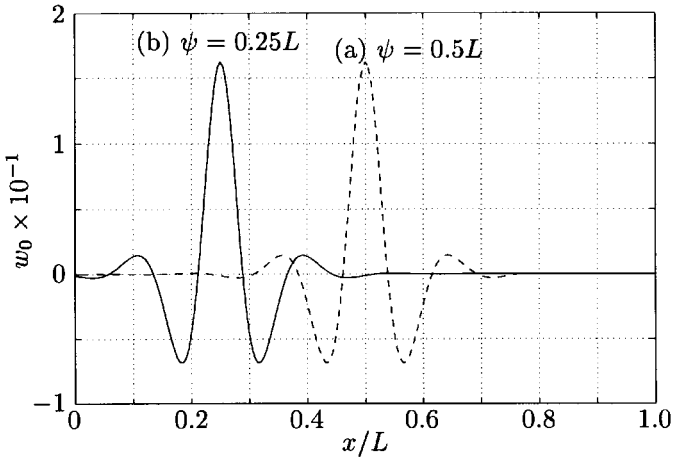

Fig. 11. Examples of ψ variation in $W_0, A_0 = 1.622 \times 10^{-1}$, $\alpha = 21.033$: (a) $\psi = 0.5L$; (b) $\psi = 0.25\,L$.

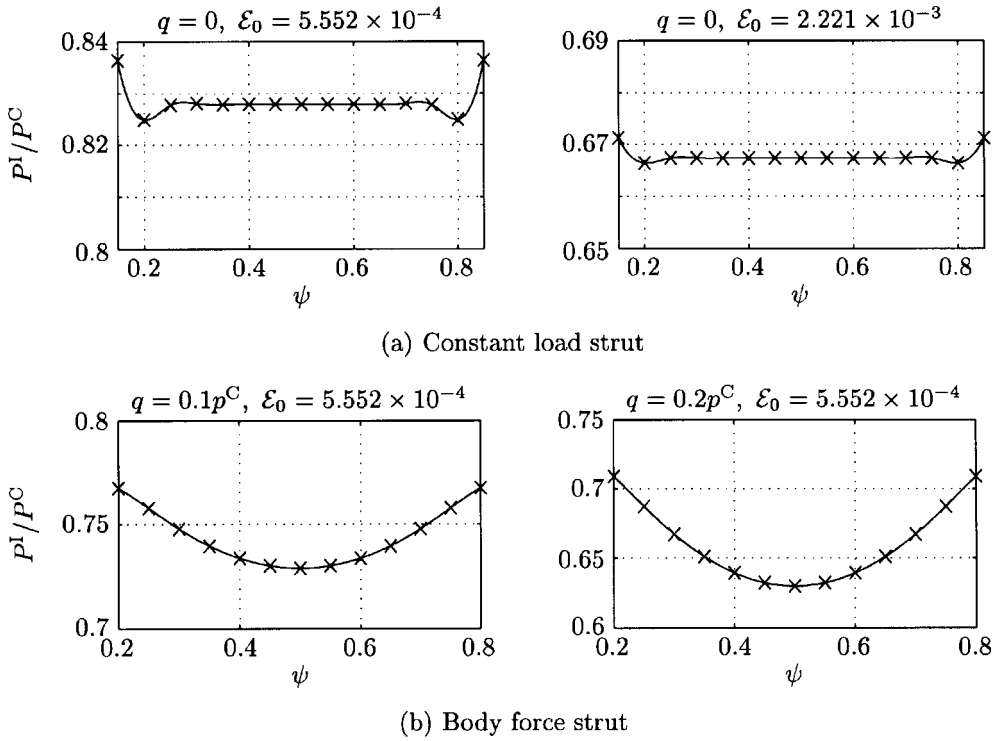

Fig. 12. Examples of ψ variations for the heuristic struts.

boundaries are less important, the limit load is invariant with respect to the location of the maximum of w_0.

Fig. 12(b) shows similar plots as Fig. 12(a) for the body force strut. It shows that the minimum limit load occurs when the maximum of the imperfection is at midspan. The bowl shape of this curve deepens as q increases. Therefore for the sandwich panel, which has been shown to share the variable stress property along the panel length of the body force model (Hunt and Wadee, 1998), we need only consider symmetric imperfections about midspan: $\psi = L/2$.

4.3. Sandwich panel

A simple optimization routine is invoked in which the objective is to maximize the linear critical load P^{C} while keeping the core volume constant. As a result, the two distinct modes of buckling, overall and local, are brought together to be triggered at the same load. The design optimum and two neighbouring case are then examined in the nonlinear post-buckling range for both the perfect and imperfect cases. The results presented are an extension of a recent paper by Wadee and Hunt (1998b).

4.3.1. Optimization of panel geometry

A practical sandwich panel is considered with the following properties as explained in Fig. 3. For the face plates: $E = 68{,}947.57$ N mm^{-2} and $v = 0.3$, with $t = 0.508$ mm and $L = 508$ mm. For the core: $E_x = E_y = 25.0$ N mm^{-2}, $G_{\mathrm{c}} = 10.9$ N mm^{-2} and $v_x = v_y = 0.2$. The core is assumed to be linearly elastic. The important constraint in the optimization is that the cross-sectional area of core material (bc)

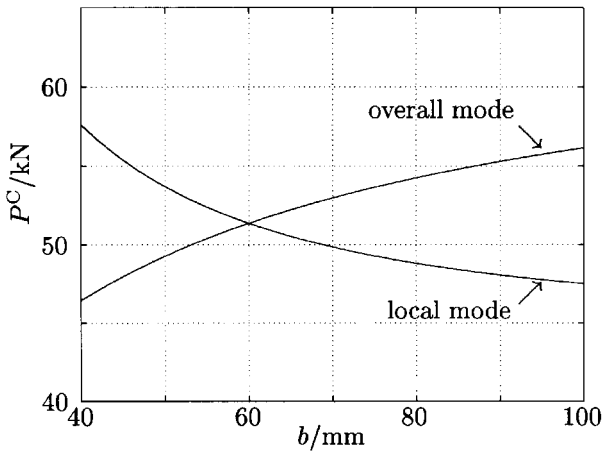

Fig. 13. Critical load variations as sandwich panel width b varies.

is constant—here $bc = 6000$ mm^2. Fig. 13 shows the variation of the critical loads as b changes. A design optimum is achieved when the maximum buckling load is found—where the curves cross.

However, such optimization schemes are known to promote nonlinear interactive post-buckling effects (Thompson and Lewis, 1972; Thompson and Supple, 1973). This is quantified by examining perfect post-buckling equilibrium paths and determining imperfection-sensitivity characteristics for the optimal case and its neighbourhood.

4.3.2. Perfect post-buckling behaviour

In this section, three separate configurations of the sandwich panel are studied. These cases cover configurations for which the overall mode is critical ($b = 50$ mm), where the modes coincide ($b = 60$ mm), and where the local mode is critical ($b = 74$ mm). The neighbouring cases to the optimum have identical critical loads. The position of the secondary bifurcation is tabulated in Table 2: this compares the periodic post-buckling model with the current localized model. It turns out that the localized model virtually has a coincident secondary bifurcation with the critical bifurcation ($\varepsilon^S/\varepsilon^C = 1$) whereas the periodic cases require a large increase in total deformation before any interactive buckling takes place. The post-buckling response predicted from the localized model for each case is shown in Fig. 14.

The plots in Fig. 14 show that the behaviour of each case is similar—all exhibiting highly unstable snapback behaviour, thereby being initially unstable in both dead and rigid loading. The proximity of ε^C and ε^S, however, is dependent on the sandwich panel geometry. Where the overall mode governs the behaviour, there is a small gap between initial overall buckling and interactively induced localized

Table 2
Comparison of relative deformation at secondary bifurcation position for periodic and localized post-buckling models

b	Periodic $\varepsilon^S/\varepsilon^C$	Localized $\varepsilon^S/\varepsilon^C$
50	2.27	1.0143
60	4.59	1.0008
74	10.25	1.0000

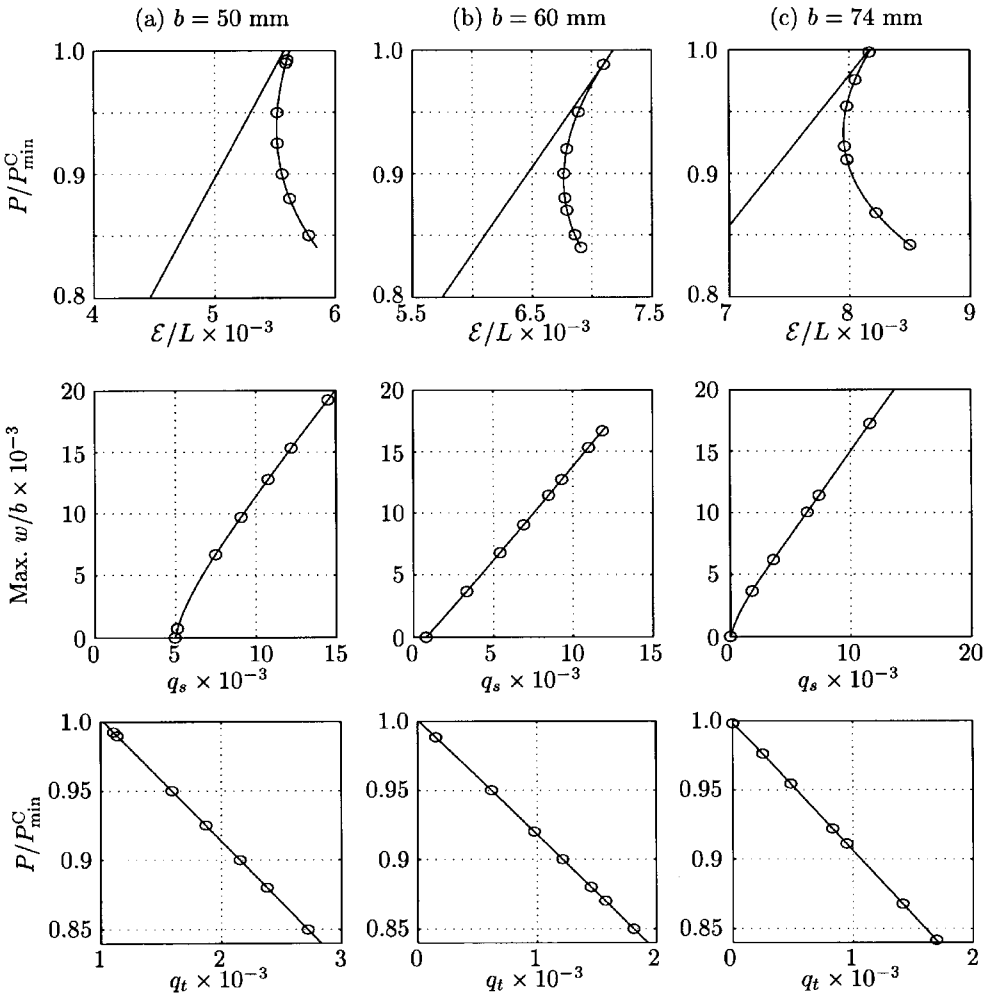

Fig. 14. Equilibrium paths and relative modal amplitudes for sandwich configurations: (a) overall mode critical: $P^{C}_{min} = P^{C}_{o}$; (b) optimum case: $P^{C}_{min} = P^{C}_{o} = P^{C}_{l}$; (c) local mode critical: $P^{C}_{min} = P^{C}_{l} = 0.922P^{C}_{o}$.

buckling, giving some warning of impending collapse. However, where the local mode governs, only a tiny overall perturbation is required to induce localization; giving negligible warning of impending collapse under dead or rigid loading conditions.

Another important variation is P against q_t (Fig. 14) because this is a guide to the respective coefficients p and q of the body force strut. Unlike the cases considered for the body force, the value of q_t varies with P, and q_t is very small when P is near critical. Thus, it is to be expected that the graphs of the worst case combination of α and A_0 intersect the origin unlike the curves shown in Fig. 10 for the different q values.

4.3.3. Imperfection-sensitivity

In this imperfection sensitivity study of the sandwich panel, as with the body force strut, varying β away from the linear eigenvalue solution has negligible effect on the limit load. However, the study of

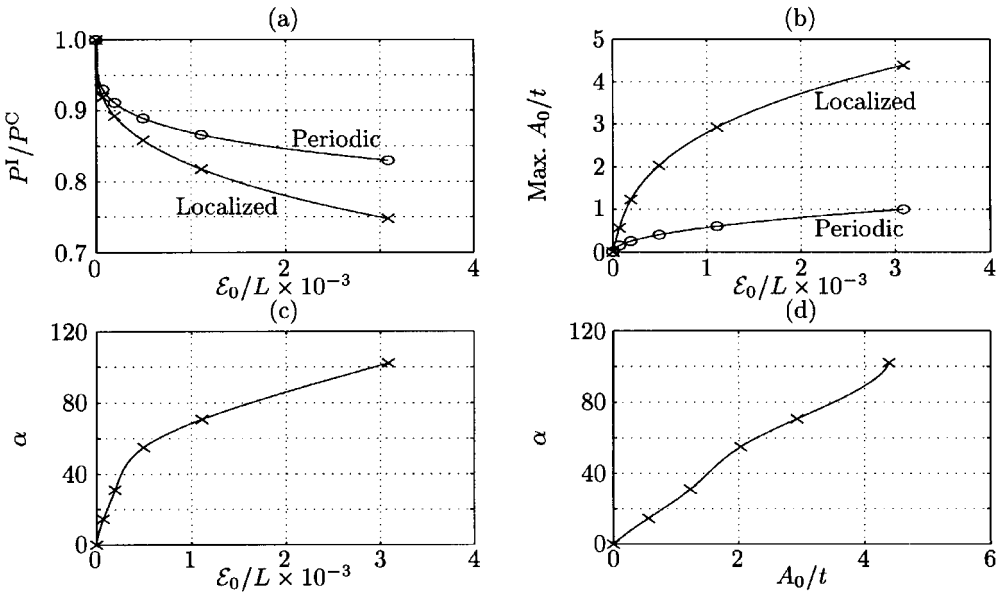

Fig. 15. Imperfection sensitivity diagrams for optimal case $b = 60$ mm: (a) limit load P^1/P^C against imperfection end-shortening ε_0/L; (b) amplitude of w_0 against ε_0/L; (c) degree of localization α against ε_0/L; (d) α against A_0/t.

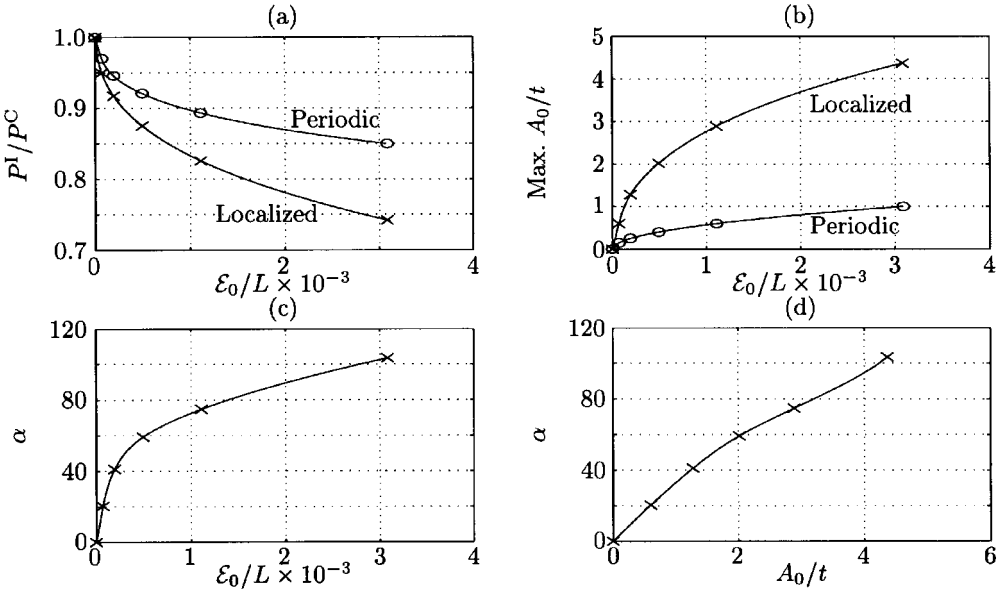

Fig. 16. Imperfection sensitivity diagrams for neighbouring case (overall mode critical) $b = 50$ mm: (a) limit load P^1/P^C against imperfection end-shortening ε_0/L; (b) amplitude of w_0, A_0/t, against ε_0/L; (c) degree of localization α against ε_0/L; (d) α against A_0/t.

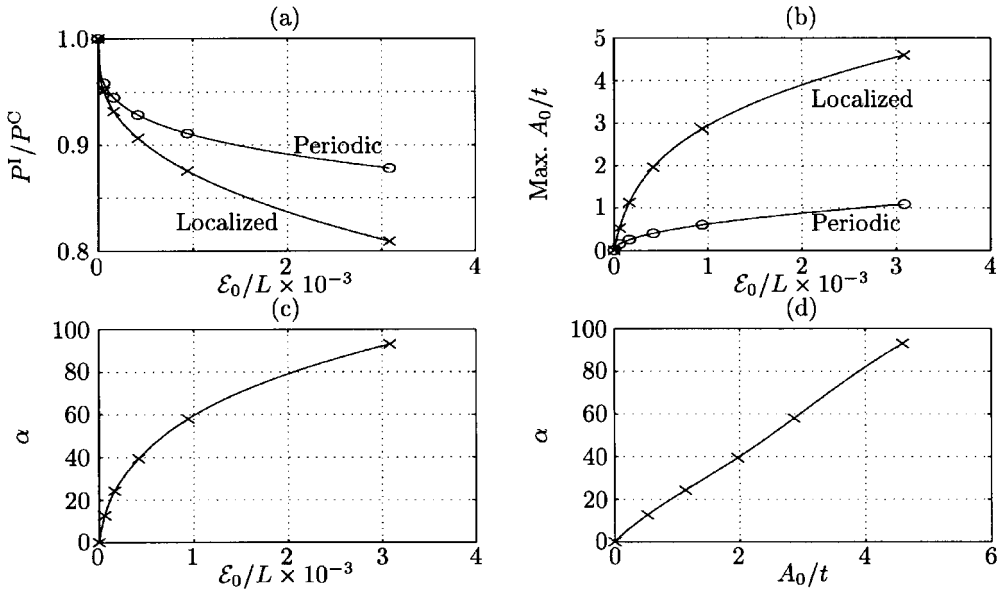

Fig. 17. Imperfection sensitivity diagrams for neighbouring case (local mode critical) $b = 74$ mm: (a) limit load P^1/P^C against imperfection end-shortening ε_0/L; (b) amplitude of w_0 against ε_0/L; (c) degree of localization α against ε_0/L; (d) α against A_0/t.

periodic imperfections is presented because of the fact that this type of imperfections may occur quite naturally from, for instance, the material manufacturing processes or in the sandwich panel construction itself (Karlsson and Åström, 1997). The initial imperfection w_0 represents displacement of one face of the panel. Investigations of the imperfection for both periodic and localized cases are performed with the same procedure as outlined for the constant load strut, except that the value of β is fixed at its linear eigenvalue solution.

Figs. 15–17 show the comparison of the imperfection-sensitivities from periodic and localized imperfections for the optimal and the neighbouring cases respectively. These plots show that for the same value of ε_0, the localized imperfection has a considerably more severe impact on the limit load than the corresponding periodic one. Also α increases monotonically with A_0 for the worst case localized imperfection. However, the sensitivities of the neighbouring cases are not quite as severe as the optimum.

The results are similar in form to the behaviour exhibited by the body force strut. The periodic imperfection is never found to be as severe as the corresponding localized case except at the secondary bifurcation. Nevertheless, it is shown that any form of imperfection on one face of a sandwich panel denies it the ability to carry its linear eigenvalue critical load; this is most severe for the optimized panel considered.

5. Concluding remarks

This study has highlighted the importance of localization in the behaviour of imperfect subcritical structural systems. In contrast to earlier work by Amazigo and his co-workers (1970; 1971) on similar systems, localized imperfections are identified as the most severe for the majority of load cases. For the strut on a softening foundation with a constant axial load, a transition point is identified; this pinpoints

the transition of the worst case imperfection from being periodic to localized. Because of its similar length dependence, the transition point seems to be related to the secondary bifurcation of the perfect case, which transforms initially periodic to localized buckling. For a similar strut but with a non-constant axial load maximized at midspan, the worst case is a localized imperfection with maximum at midspan—the body force strut and the axially-loaded sandwich panel occupy this category.

In the case study of a practical sandwich panel, optimized via coincidence of distinct linear modes, a heightened imperfection-sensitivity is observed in the optimal case. Initial small local deformation is shown to have a significant reduction in the real (imperfect) axial load capacity. This should sound a note of caution for designers; the optimized panel and the neighbouring cases all show unstable snap-back behaviour not predicted by earlier periodic Rayleigh–Ritz approximations of post-buckling. Thus, not only does the localization phenomenon drive post-buckling to be much less stable in an optimal case, but it also severely exaggerates the imperfection-sensitivity characteristic.

Acknowledgements

Financial support for the author was provided by a University of Bath Studentship.

References

Allen, H.G., 1969. Analysis and Design of Structural Sandwich Panels. Pergamon Press, Oxford.

Amazigo, J.C., Fraser, W.B., 1971. Buckling under external pressure of cylindrical shells with dimple shaped initial imperfections. Int. J. Solids Struct. 7, 883–900.

Amazigo, J.C., Budiansky, B., Carrier, G.F., 1970. Asymptotic analyses of the buckling of imperfect columns on nonlinear elastic foundations. Int. J. Solids Struct. 6, 1341–1356.

Budiansky, B. (Ed.), 1976. Buckling of Structures. IUTAM Symposium, Cambridge, U.S.A., 1974. Springer, Berlin.

Champneys, A.R., Hunt, G.W., Thompson, J.M.T., 1997. Localization and solitary waves in solid mechanics. Phil. Trans. R. Soc. Lond. A 355 (1732), 2073–2213.

Doedel, E.J., Wang, X.J., Fairgrieve, T.F., 1995. AUTO94: Software for continuation and bifurcation problems in ordinary differential equations. Technical Report CRPC-95-2, California Institute of Technology.

Heck, A., 1996. Introduction to Maple. Springer, New York.

Hunt, G.W., Wadee, M.A., 1998. Localization and mode interaction in sandwich structures. Proc. R. Soc. Lond. A 454 (1972), 1197–1216.

Hunt, G.W., Bolt, H.M., Thompson, J.M.T., 1989. Structural localization phenomena and the dynamical phase-space analogy. Proc. R. Soc. Lond. A 425 (1869), 245–267.

Hunt, G.W., Da Silva, L.S., Manzocchi, G.M.E., 1988. Interactive buckling in sandwich structures. Proc. R. Soc. Lond. A 417 (1852), 155–177.

Karlsson, K.F., Astrom, B.T., 1997. Manufacturing and applications of structural sandwich components. Composites Part A 28A (2), 97–111.

Kodiyalam, S., Nagendra, S., DeStefano, J., 1996. Composite sandwich structure optimization with application to satellite components. AIAA J 34 (3), 614–621.

Lord, G.J., Champneys, A.R., Hunt, G.W., 1997. Computation of localized post-buckling in long axially-compressed cylindrical shells. Phil. Trans. R. Soc. Lond. A 355 (1732), 2137–2150.

Lucena Neto, E., 1992. Localized post-buckling solutions in long axially-compressed cylindrical shells. Ph.D. thesis, Imperial College of Science, Technology and Medicine, London.

Mróz, Z., 1970. Optimal design of structures of composite materials. Int. J. Solids Struct. 6, 859–870.

Prager, W., 1968. Optimality criteria in structural design. Proc. Nat. Acad. Sci 61, 794–796.

Steven, G.P., Querin, O.M., Guan, H., Xie, Y.M. (Eds.), 1998. Structural optimisation. Proceedings of the Australasian Conference on Structural Optimisation. Oxbridge, Victoria, Australia.

Thompson, J.M.T., Hunt, G.W., 1973. A General Theory of Elastic Stability. Wiley, London.

Thompson, J.M.T., Hunt, G.W., 1984. Elastic Instability Phenomena. Wiley, Chichester.

Thompson, J.M.T., Lewis, G.M., 1972. On the optimum design of thin-walled compression members. J. Mech. Phys. Solids 20, 101–109.

Thompson, J.M.T., Supple, W.J., 1973. Erosion of optimum designs by compound branching phenomena. J. Mech. Phys. Solids 21, 135–144.

Wadee, M.A., Hunt, G.W., 1998a. Interactively induced localized buckling in sandwich structures with core orthotropy. Trans. ASME J. Appl. Mech. 65 (2), 523–528.

Wadee, M.A., Hunt, G.W., 1998b. Nonlinear interaction and localization in sandwich structures: a case of optimization promoting complex instability. In: Steven et al. (1998), pp. 189–196.

Wadee, M.K., Hunt, G.W., Whiting, A.I.M., 1997. Asymptotic and Rayleigh–Ritz routes to localized buckling solutions in an elastic instability problem. Proc. R. Soc. Lond. A 453 (1965), 2085–2107.